

Neutral Beam Injection Studies for W VII AS
using the 3-D Computer Code FAFNER

G.G.Lister, F.P.Penningsfeld, W.Ott, and E.Speth
Max-Planck-Institut für Plasmaphysik, EURATOM Association
D-8046 Garching, Federal Republic of Germany

ABSTRACT

Results of 3-D numerical computations predicting deposition profiles, shine through and fast ion orbit losses for neutral injection experiments in the W VII-AS stellarator are presented. For 40 keV H injection into D plasma, total power losses are restricted to $\sim 10\%$ over a wide range of plasma parameters and significant heating (~ 2 W/cc for 1.5 MW injected power) is predicted.

1. INTRODUCTION

Following the success of neutral beam heating experiments in sustaining currentfree plasmas in the W VII-A stellarator /1/, a new experiment, W VII-AS /2/, is planned in which the helical windings will be replaced by modular coils. Suitable modification of these coils at the neutral beam entry ports will permit the beams to be injected tangentially to the magnetic field. Losses due to shine through or trapping in local magnetic field ripples are thus minimised.

The total injected power projected for the first phase of W VII-AS is 1.5 MW, which will be obtained using 4 periplasmatron sources /3/ of the type currently used on ASDEX. This power may be doubled if the full beam-lines with 8 sources were used.

Results presented in this paper are for plasma parameters extrapolated from W VII-A results /4/. We discuss the effects of plasma density and injection energy on the expected heating efficiency and show power deposition profiles for typical cases.

2. THE NEUTRAL BEAM-PLASMA SYSTEM

W VII-AS will be a stellarator of major radius 200 cm, effective minor radius 22 cm, toroidal magnetic field 3 T and external iota of between 0.25 and 0.6 (normal operating value 0.4). The neutral beam system and the target plasma are illustrated in Fig. 1. L_1, L_2, L_1', L_2' , each represent a pair of vertically stacked sources, placed equidistant from the mid plane of the torus, and directed at an angle $\pm 2.86^\circ$ to the horizontal. Sources L and L' are oppositely directed, to prevent toroidal plasma rotation and to cancel beam driven currents. It was found that the optimum radius of tangency for sources L_1, L_1' is $R_1 = 191$ cm, which restricts that for the set L_2, L_2' to $R_2 = 164$ cm.

Cross sections of the target plasma in different azimuthal planes ϕ are also illustrated in Fig.1, onto which have been superposed neutral particle contours from the two sources L_1 in these planes. In the region where the beams enter the plasma, the lines of equal magnetic flux are relatively close together, and hence fast ion deposition in the plasma is highly sensitive to the choice of density profiles.

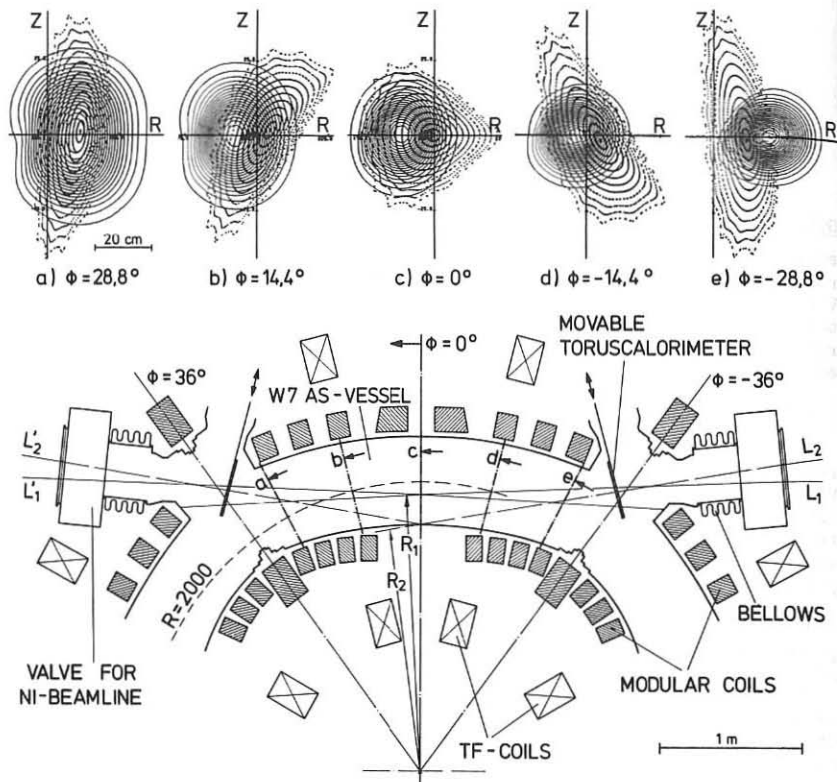


Fig. 1: W VII-AS injection geometry and cross sections of beam and plasma

3. NUMERICAL METHODS AND PLASMA PROFILES

Standard Monte Carlo methods have been used to model the trapping of neutral particles and the subsequent interaction of the resulting fast ions with the plasma /5/. A new code, FAFNER /6/ has been constructed to include the 3-dimensional plasma and a more detailed description of the beamline, necessary in view of the comparable dimensions of the plasma and beam cross sections. The magnetic field configuration is modelled by a set of coefficients supplied by Dommaschk /7/.

The plasma density and temperature profiles are given as a function of the flux function s , defined as the distance from the plasma axis along the line $z=0$ (torus mid plane) in the $\phi=0$ plane, where the plasma is approximately triangular. Each point in the plasma will thus have a defined density and temperature by a suitable coordinate transformation into the $\phi=0$ plane. Profiles used to obtain results presented in this paper are:

$$n_e = n_e(0)/(1+(s/b)^6) \quad b = 12 \text{ cm}$$

$$T_e = T_e(0) \cdot (1-(s/a)^2) \quad a = 22 \text{ cm.}$$

The absolute values for $n_e(0)$ and $T_e(0)$ were obtained from transport simulations /4/.

4. RESULTS AND CONCLUSIONS

Results of computations are shown in Figs. 2-5. In Fig. 2 computed fractional orbit losses, shine through losses (a and b) and heating power fractions to ions p_i and electrons p_e versus central electron density $n(0)$ are plotted.

A comparison is made between inner (L_1) and outer (L_2) sources of shine through losses for different densities. Clearly, losses in the low density ECRH generated plasma ($n_e(0) = 4 \times 10^{13} \text{ cm}^{-3}$) using the inner sources would prove acceptable. We also show expected losses, and the fraction of power given to plasma ions and electrons from sources L_1 and L_1' . As expected, there is a slight increase in orbit losses for higher densities, due to the higher fraction of fast ions born near the plasma edge, but this is partially compensated by the reduction in shine through losses, resulting generally in a power loss of $\approx 10\%$. The plasma electrons receive an increased share of the available power for higher density, due to the lower T_e with increasing density /4/.

Figure 3 shows power deposition profiles (to ions and electrons) versus effective radius, for a high density, $n_e(0) = 2 \times 10^{14} \text{ cm}^{-3}$ plasma. The ions in the central plasma receive $\approx 1 \text{ W/cc}$ power and the electrons $\approx 1 \text{ W/cc}$, assuming a total injected power of 1.5 MW.

Figures 4 and 5 illustrate the effect of varying the injection energy over a range of 20 to 50 keV. For high density plasmas differences between 40 and 50 keV injection are not statistically significant. However, 30 keV injection would result in a markedly poorer performance. Deposition profiles, illustrated in Fig. 4, show a marked central hollow, and orbit losses increase from 5% to 12%, due to the reduced penetration of the beam for lower energies. Increase of E_0/E_C (E_0 is injection energy, E_C is "critical energy"), however, results in a lower fraction of power delivered directly to the ions (Fig. 5).

REFERENCES

- /1/ W VII A-Team, NI-Team, 9th Conf. Plasma Phys. Contr. Nucl. Fusion Res., Baltimore, 1982, paper IAEA-CN-41/L5
- /2/ Broßmann, U., Dommasch, W., Herrnegger, F., Grieger, G., Kißlinger, J., Lotz, W., Nührenberg, H., Rau, F., Renner, H., Ringler, H., Sapper, J., Schlüter, A., Wobig, H.; *ibid*; Paper IAEA-CN-41/Q5
- /3/ Bonnal, J.F., Bracco, G., Bussac, J.P., Druaux, J., Oberson, R., Romain, R. Proc. 8th Symp. Engin. Probl. Fus. Res., San Francisco, 1979, Vol. II, 1056
- /4/ Wobig, H., to be published
- /5/ Goldston, R., McCune, D.C., Towner, H.H., Davis, S.L., Hawryluk, R.J., and Schmidt, G.L., J. Comp. Phys. 43, 1981, 65
- /6/ Lister, G.G., to be published
- /7/ Dommasch, W., 1978, IPP-Report 0/38.

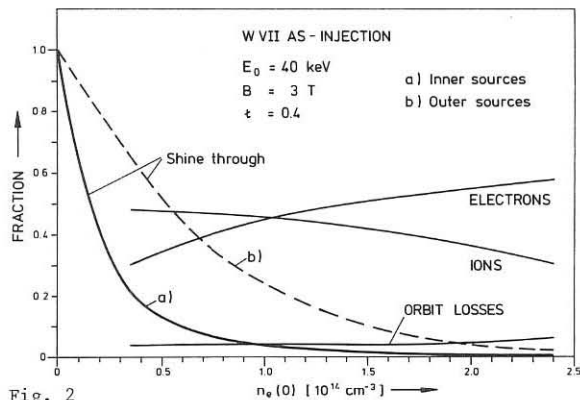


Fig. 2

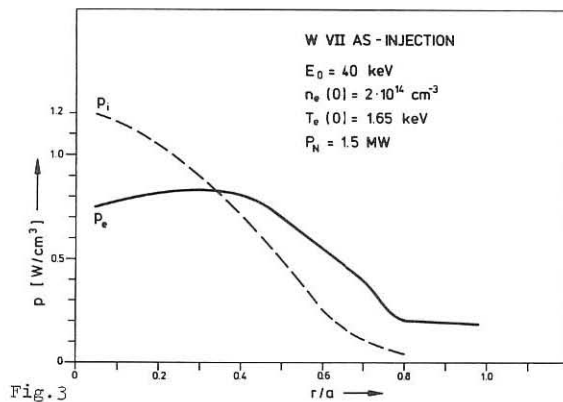


Fig. 3

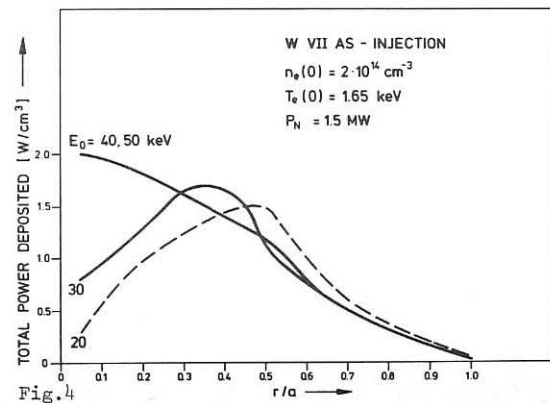


Fig. 4

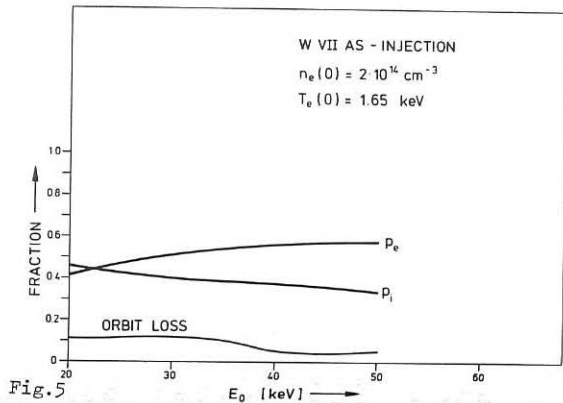


Fig. 5